UDC 661.183.124:628.316.12:[546.56](045)
DOI: 10.15587/2706-5448.2024.314231

Junjie Yu,
Viktoriia Tobilko

ADSORPTION REMOVAL OF COPPER(II) FROM WATER BY ZERO VALENT IRON LOADED DENDRITIC MESOPOROUS SILICA

The object of research is synthesized dendritic mesoporous nanoscale silica (DMSN) modified with zero-valent iron (Fe^0@DMSN). This material exhibits a high adsorption capacity for heavy metal ions, in particular copper, whose increased content in the aquatic environment poses a threat to living organisms. In this regard, the main physicochemical features of the removal of copper cations from the aqueous medium using the obtained sample were investigated.

The morphology of the obtained dendritic silicas was studied by electron microscopy and the presence of a layer of zero-valent iron was confirmed by X-ray diffraction analysis and infrared spectroscopy. The parameters of the porous structure of the synthesized materials were determined. It was found that after modification of mesoporous silica with particles of zero-valent iron, the value of its specific surface area decreased from 504 m^2/g to 312 m^2/g. This may be due to the formation of a Fe^0 layer not only on their surface but also in the channels of the inorganic matrix, which has a unique dendritic structure characteristic of this type of particles. At the same time, the number of active centers increases due to the enrichment of the silica surface with functional modifier groups that show a high affinity for metal cations.

The adsorption capacity of Fe^0@DMSN towards Cu^{2+} ions has been studied and it has been shown that the maximum adsorption value is 39.8 mg/g, which is significantly higher than that of the initial synthesized DMSN sample (0.7 mg/g).

The experimental data obtained indicate that the obtained sorption material based on dendritic mesoporous silica nanoparticles with a layer of reactive zero-valent iron can be used for the purification of water contaminated with metal ions. In addition, the magnetic properties of such materials, known and proven by various scientists, will make it easy to separate the solid phase in the processes of sorption water purification using magnetic separation.

Keywords: *DMSN, mesoporous silica, modification, adsorption, water treatment, heavy metals.*

Received date: 14.09.2024
Accepted date: 29.10.2024
Published date: 31.10.2024

How to cite
Yu, J., Tobilko, V. (2024). Adsorption removal of copper(II) from water by zero valent iron loaded dendritic mesoporous silica. Technology Audit and Production Reserves, 5 (3 (79)), 6–12. https://doi.org/10.15587/2706-5448.2024.314231

1. Introduction

In recent years, with the fast development of urbanization and infrastructure around the world, a large amount of industrial waste has been discharged into the municipal wastewater system along with wastewater. Some modern technologies are applied to solve this problem, such as the use of filtration systems to remove solid waste from wastewater. However heavy metals in wastewater are mixed into the water body in ionic form and are difficult to remove [1, 2]. This wastewater contains a large amount of copper(II), and studies have shown that the copper ion content in the water body will seriously affect the self-purification function of the water body. The World Health Organization (WHO) has set the limit for copper ion concentration in natural waters at 3.0 mg/l [3].

Meanwhile, these heavy metals entering the ecosystem will continue to be enriched through the biological chain because they cannot be decomposed. They are eventually absorbed by the human body, thus causing damage to the internal organs of the human body (e. g., liver, kidneys) and leading to the occurrence of various types of chronic and acute diseases [4].

At present, in order to solve the problem of heavy metal ion pollution in wastewater, scientists have made various attempts, including ion exchange, electrolysis, membrane filtration, photocatalytic and adsorption methods, etc. [5–9]. Among these methods, the adsorption method has attracted much attention due to its simplicity, efficiency, and high operability. However, traditional adsorbents, such as activated carbon, often need to be used in large quantities due to their low adsorption capacity, resulting in high actual adsorption cost, which is not conducive to large-scale industrialization. Therefore, the search for a cost-appropriate and efficient adsorbent for heavy metals in water is crucial for large-scale industrial application

of adsorption methods. Many attempts have been made to find alternatives to traditional adsorbents. For example, in [10] conducted adsorption experiments on copper ions in wastewater using acid-modified bagasse. The results showed that the efficiency of bagasse in removing Cu(II) from synthetic and industrial wastewater was comparable to that of traditional activated carbon materials, but the cost was over 10 times lower than that of traditional activated carbon materials.

In recent decades, silica materials have been widely studied due to their good thermal stability as well as their surface polyhydroxyl groups, chemical stability, etc. [11], In order to enhance the ability of silica to adsorb heavy metals from wastewater researchers have used a number of different approaches. These approaches include using different silica sources and synthetic solvents to modify its size and shape, so that the structure of silica becomes more conducive to adsorption [12, 13], or enhancing the ability to adsorb pollutants through functional groups on the surface of modified silica or by complexing it with other materials [14, 15]. Recently, the authors of [16] successfully prepared silica materials with dendritic morphology by an anion-assisted method. This dendritic silica nanomaterial has a larger surface area and internal pores, which offers a natural advantage for heavy metal adsorption in water.

In this work, to solve the drawbacks of the dendritic silica material's weak inherent ability to capture heavy metal ions in the water body, as well as the difficulty of solid-liquid separation after adsorption, let's introduce zero-valent iron as an additional adsorption site on the surface of the dendritic silica. The specific operation is as follows: the dendritic silica material is immersed in Fe^{3+} solution, and the Fe^{3+} ions are reduced by sodium borohydride solution under a nitrogen atmosphere so that the reduced Fe^0 is successfully loaded onto the silica surface. The silicon dioxide substrate can make the reduced Fe^0 firmly adhere on the surface of dendritic silica through electrostatic attraction, which makes it more stable; while the loading of Fe^0 provides more additional heavy metal adsorption sites for the composite material.

Therefore, *the aim of this research* is to obtain an adsorbent based on mesoporous silica with the morphology of dendritic nanosized particles and an active layer of zero-valent iron for the removal of heavy metal ions from aqueous solutions. The study of the main physicochemical characteristics and sorption properties of the obtained materials will allow the synthesis of adsorbents with controlled structure parameters, which will significantly increase the efficiency of their use in the environmental field.

2. Materials and Methods

2.1. Materials. *The object of the study* is synthesized dendritic mesoporous nanoscale silica (DMSN) modified with zero-valent iron (Fe^0@DMSN).

Cetyltrimethylammonium bromide (CTAB), triethanolamine (TEA), tetraethoxysilane (TEOS), sodium salicylate (NaSal) and Sodium Borohydride ($NaBH_4$) were purchased from MERCK, Germany. Iron(III) chloride hexahydrate ($FeCl_3{\cdot}6H_2O$) and Ethanol (EtOH) were purchased from CHEMLABORREACTIV LLC (Ukraine). Distilled water was used throughout all experiments. All chemicals used in this work were in analytic grade and used without further purification.

2.2. Instruments and analytic methods. The materials were characterized using various techniques. Scanning Electron Microscope (SEM) images and EDS mapping patterns were obtained using Nova Nano SEM450 manufactured by FEI (USA), confirming the successful composite of Fe^0 nanoparticles with DMSN with uniform elemental distribution. High-resolution TEM images were tested using a JEM-2010F model transmission electron microscope, (Japan), at an accelerating voltage of 200 kV to obtain a high-resolution structure of the material. The crystal structure of the prepared materials was analyzed by diffraction using Cu-Kα rays with a D8 Advance X-ray diffractometer (XRD) manufactured in Germany. Information such as functional groups of the materials was obtained by Fourier transform infrared spectroscopy (FTIR) measurements (scanning in the wavelength range of 4000–500 cm^{-1}) using a Bruker Vertex 70 model (made in Germany) infrared spectrometer. The method of low-temperature (–196 °C) nitrogen adsorption-desorption was used to study the surface parameters and porous structure of the synthesized samples. The samples were degassed in a vacuum before the measurement. The data obtained were processed using specialized software Quantachrome NovaWin version 11.04. The specific surface area (S_{BET}, m^2/g) was calculated by the Brunauer-Emmett-Teller (BET) multipoint method, and the external pore surface (S_{ext}, m^2/g) and micropore surface (S_{micro}, m^2/g) were estimated by the t-method. The total pore volume (V_Σ, cm^3/g) was determined by the maximum adsorbed volume of nitrogen at a relative pressure $p/p_0 \approx 1$ (0.99). The micropore volume (V_{micro}, cm^3/g) was estimated by the t-method, and their percentage content (V_m, %) was calculated using the following formula:

$$V_m = \frac{V_{micro}}{V_\Sigma} \cdot 100, \quad (1)$$

where V_{micro} and V_Σ (cm^3/g) are the micropore and total pore volumes of synthesized samples, respectively.

The average pore radius (R, nm) was calculated using the following formula:

$$R = \frac{2V_\Sigma}{S_{BET}}, \quad (2)$$

where V_Σ (cm^3/g) and S_{BET} (m^2/g) are the total pore volume and the specific surface area of synthesized samples, respectively.

All adsorption experiments were performed under static conditions at 25±2 °C. Solutions containing 10 mg of adsorbent and 50 ml of heavy metal ions were placed in a shaker (Biosan OS-20, Latvia) and shaken continuously for 1 hour. After adsorption equilibrium was established, the adsorbent and liquid phase were separated by centrifugation (3600 rpm) and the Cu^{2+} concentration in the supernatant was determined by ICP-OES (Thermo Scientific iCAP 7400 ICP-OES, USA).

The value of the adsorption value (a, $mg{\cdot}g^{-1}$) was calculated according to the formula:

$$a = \frac{(C_{in} - C_e) \cdot V}{m}, \quad (3)$$

where C_{in}, C_e – initial and equilibrium metal concentration, mg/dm^3; V – solution volume, dm^3; m – the weight of the sorbent, g.

ISSN 2664-9969

The removal efficiency (X, %) of copper ions were estimated according to the formula:

$$X(\%)=\frac{C_{in}-C_{eq}}{C_{in}}\cdot 100, \quad (4)$$

where C_{in}, C_{eq} are representing the initial and equilibrium copper(II) ions concentrations (mg/md^3).

2.3. Preparation of dendritic mesoporous silica nanoparticles (DMSN). The dendritic mesoporous silica nanoparticles (DMSN) were synthesized by a one-pot method using CTAB and NaSal as structure-directing agents, TEOS as the silica source, and TEA as a catalyst according to a reported method with slight modifications [17, 18]. In a typical process, 1.36 g of TEA was dissolved in 500 ml of water under magnetic stirring for 5 minutes. The solution was transferred into a water bath set at 80 °C. After uniform stirring for 30 minutes, 7.6 g of CTAB and 3.36 g of NaSal were weighed out. These compounds were added to the reaction container and stirring continued for an additional hour. The as-prepared solution mixture, consisting of 80 ml of TEOS and 10 ml of ethanol, was added dropwise into the reaction container using a peristaltic pump. This mixture was added over 30 minutes with constant stirring. Stirring continued at 80 °C for 1.5 hours after the completion of dropwise addition. After that, the obtained product was washed three times with water and ethanol to remove impurities from the supernatant. The white product settled at the bottom layer was kept. Finally, the collected product was calcined at 550 °C for 6 hours to remove the structure-directing agents. This product was labeled as DMSN.

2.4. Preparation of Fe^0@DMSN. Zero-valent iron supported by dendritic mesoporous silica nanoparticles was synthesized according to a reported method with slight modifications [19]. The DMSN sample was mixed with a solution of $FeCl_3{\cdot}6H_2O$ of a certain concentration and stirred for 30 minutes on a magnetic stirrer. The mass ratio of Fe^0 to DMSN was 0.2:1. The resulting suspension (pH=2) was quantitatively transferred to a three-neck flask and the process of reducing Fe^{3+} ions with 0.1N sodium borohydride solution under a nitrogen atmosphere was carried out. After that, the obtained composite (Fe^0@DMSN) was separated from the liquid phase by centrifugation and washed three times with alcohol. The resulting precipitate was dried under vacuum at 60 °C and ground to a fraction of ≤0.1 mm.

3. Results and Discussion

Fig. 1, *a*, *b* show the SEM patterns of DMSN and Fe^0@DMSN, and it is possible to see that the DMSN material still maintains the dendritic morphology before and after Fe^0 loading and the material is well dispersed with a diameter of around 200 nm. It is also observed that its monodispersed distribution and internal mesoporous structure give it a larger specific surface area and more active sites compared to the traditional silica material, which will play a positive role in the adsorption capacity of the material. In Fig. 1, *b*, the synthetic Fe^0 loaded on the edge of DMSN can be observed in the form small particles.

To further observe the microscopic morphology of Fe^0@DMSN materials and the loading state of Fe^0, let's perform transmission electron microscopy (TEM) tests on Fe^0@DMSN, and in the TEM patterns in Fig. 1, *c*, *d*, it is possible to see that Fe^0 is tightly adhered to the surface of DMSN and aggregated into clusters to a small extent, which is due to the van der Waals forces and magnetic properties of Fe^0 nanoparticles, the unsupported Fe^0 tends to aggregate together [20]. In addition, aggregated Fe^0 material is not observed in the blank area of Fig. 1, *c*, indicating that Fe^0 is successfully composited with DMSN and firmly linked together, rather than simply stacking.

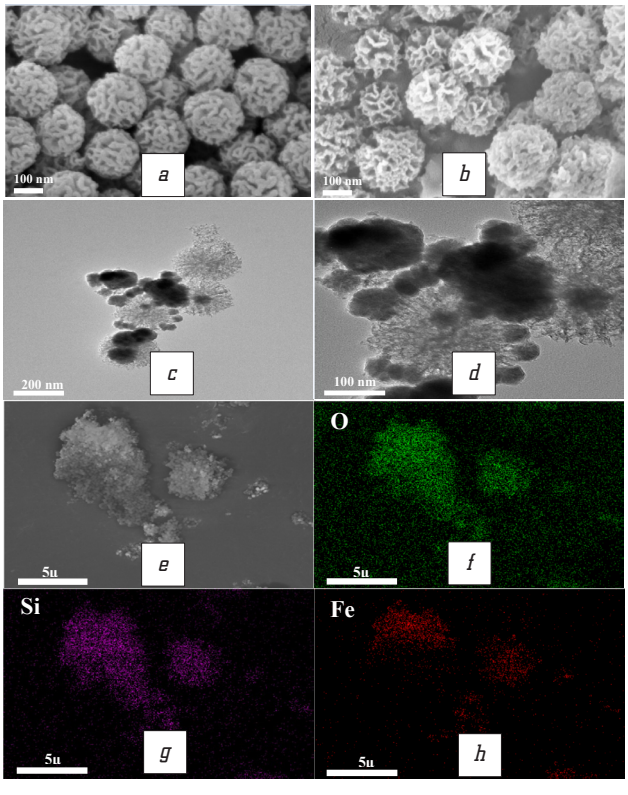

Fig. 1. Characterization of the obtained materials: *a* – SEM images of DMSN; *b* – SEM images of Fe^0@DMSN; *c*, *d* – TEM image of Fe^0@DMSN; *e*, *f*, *g*, *h* – EDS mapping characterization of Fe^0@DMSN

To observe the elemental distribution in the composites, the elemental distribution mapping test was carried out for Fe^0@DMSN in Fig. 1, *e*–*h*, and the results of the mapping test can be observed that the elements O, Si, and Fe are uniformly distributed in the materials, which further indicates the successful synthesis of Fe^0@DMSN composites.

X-ray diffraction analyses of DMSN and Fe^0@DMSN were carried out in Fig. 2. A distinct broad peak was observed at around $2\theta=24$ which is typical for amorphous silica materials. In the XRD pattern of the composite material Fe^0@DMSN, in addition to the observed broad diffraction peaks belonging to amorphous silica, two sharp peaks belonging to the (110) and (200) crystalline surfaces of Fe^0 are also revealed at $2\theta=44.7$ and $2\theta=65.0$, which is in agreement with the XRD card PDF#06-0696 of Fe^0. The above results indicate that the Fe^0 is well crystallized and loaded onto the DMSN material, and the Fe^0@DMSN composite was successfully synthesized.

The surface functional group structures of DMSN and Fe^0@DMSN were tested by FTIR spectroscopy, the results of which are shown in Fig. 3, where both materials show peaks at 3433, 1630, and 803, which corresponds to the

-OH telescopic vibration, Si-H_2O bending vibration, and O-Si-O bending, respectively. In particular, after the composite Fe^0 the Si-OH bending vibration peak at 960 cm^{-1} disappears in the FTIR spectra of Fe^0@DMSN, which may be attributed to the chemical bonding of Si-OH on the surface of DMSN with the iron atoms on the surface of Fe^0 to form Si-O-Fe [21]. In addition, the Si-O-Si vibration of the composite is red-shifted from 1100 to 1083 further indicating that the functional group structure of DMSN has changed. All these results indicate that Fe^0 was successfully dispersed in DMSN.

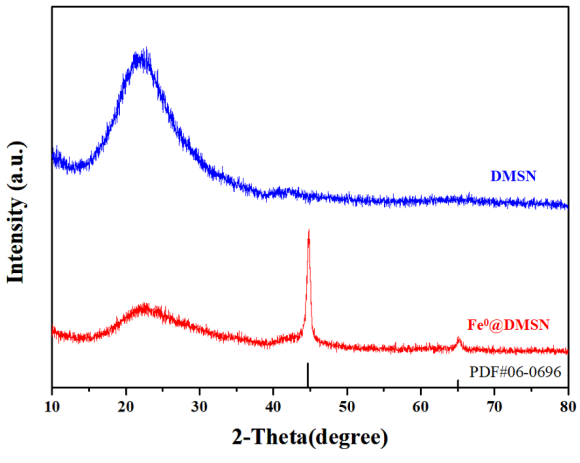

Fig. 2. XRD images of DMSN (blue line) and Fe^0@DMSN (red line)

The obtained isotherms of low-temperature nitrogen adsorption/desorption (Fig. 4, *a*) of the studied samples belong to the type IV isotherms according to the IUPAC classification with a hysteresis loop of type H3, which is typical for mesoporous materials. The value of the specific surface area for the modified sample is almost half that of the synthesized SiO_2, which may be due to the fact that nZVI occupies or partially blocks the SiO_2 pore channels. The parameters of the porous structure are presented in Table 1. The total pore volume has a similar trend. The distribution of pores by size (Fig. 4, *b*) shows a wide range of pore sizes in the range of 3–50 nm.

In the adsorption reaction, the pH of the solution affects the functional groups of the adsorbent and the solution's heavy metal ions, which in turn affects the actual adsorption effect of the adsorbent on the heavy metal solution. In Fig. 5, *a*, the adsorption capacity of Fe^0@DMSN for copper ions was tested at different pH (3~6), and the result shows that the composite material has the best adsorption effect when pH is equal to about 5, and the removal rate of copper ions in solution reaches 95.5 %. Fig. 5, *b* shows the distribution of copper ion forms in aqueous medium depending on pH (calculated using the software "The software Chemical Equilibrium Diagrams", Sweden) [22].

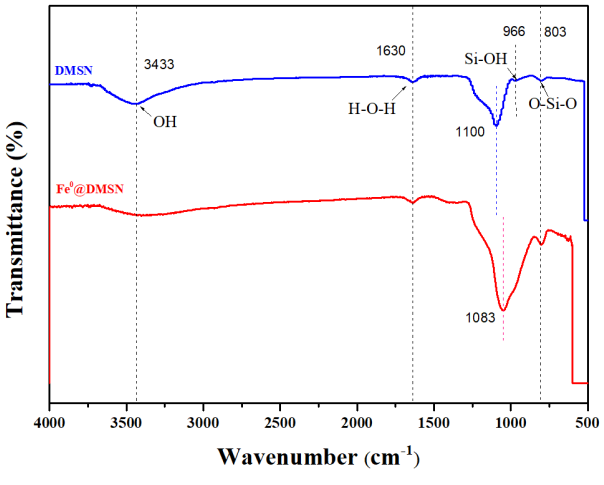

Fig. 3. FTIR images of DMSN (blue line) and Fe^0@DMSN (red line)

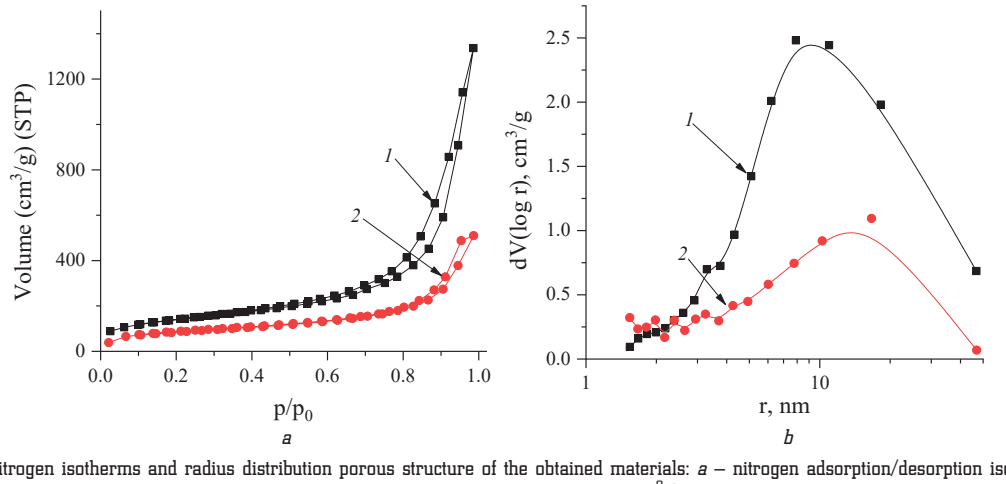

Fig. 4. Nitrogen isotherms and radius distribution porous structure of the obtained materials: *a* – nitrogen adsorption/desorption isotherms; *b* – pore radius distribution; 1 – DMSN, 2 – Fe^0@DMSN

Table 1

Parameters of the porous structure of the investigated samples

Sample	S_{BET}, m^2/g	S_{ext}, m^2/g	S_{micro}, m^2/g	V_Σ, cm^3/g	V_{micro}, cm^3/g	V_m, %	R, nm
DMSN	504	448	56	2.067	0.017	0.82	8.2
Fe^0@DMSN	312	251	61	0.788	0.021	2.66	5.1

Notes: S_{BET}, m^2/g – the specific surface area; S_{ext}, m^2/g – the external pore surface; S_{micro}, m^2/g – the micropore surface; V_Σ, cm^3/g – the total pore volume; V_{micro}, cm^3/g – the micropore volume; V_m, % – the percentage content of micropore; R, nm – the pore radius

ISSN 2664-9969

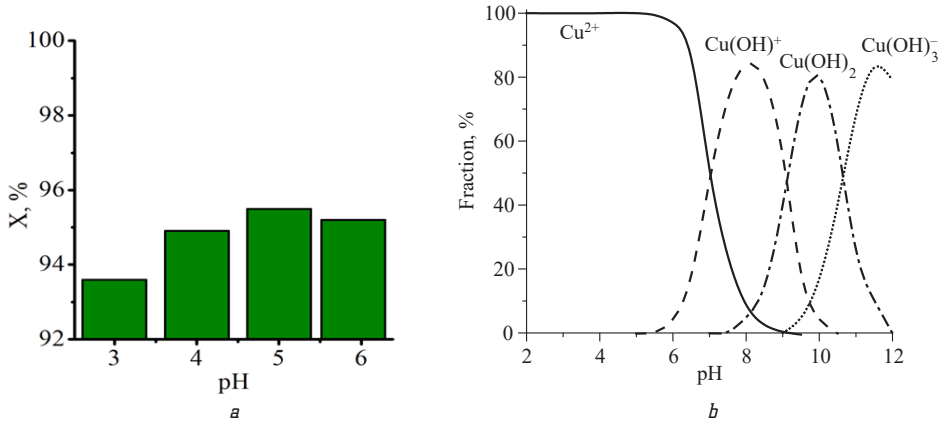

a *b*

Fig. 5. Results of adsorption of Cu^{2+} by Fe^0@DMSN under different pH: *a* – adsorption efficiency of Cu^{2+} by Fe^0@DMSN under different pH (T=298 K, $C_0(Cu^{2+})$=20 mg/l, t=2 h); *b* – diagram of the distribution of copper ion forms in aqueous medium depending on pH

In an acidic environment (pH < 6), copper is found mainly in the form of positively charged Cu^{2+} ions. When the pH shifts towards an alkaline environment, copper is precipitated in the form of hydroxides. This is the reason for the subsequent adsorption process, the solution pH was kept at 5.7±0.1.

The adsorption efficiency of Fe^0@DMSN with Cu^{2+} was investigated using adsorption kinetics Fig. 6, *a*, which showed that the composite reached equilibrium for the adsorption of Cu^{2+} ions at around 120 min. The kinetic data were fitted with pseudo-first and pseudo-second-order kinetic equations. According to the calculated constants (Table 2), the correlation coefficient of the pseudo-first-order kinetic model (R^2=0.972) is higher than that of the pseudo-second-order kinetic model (R^2=0.951), and the experimental value (q_e) is close to that calculated from the pseudo-second-order kinetic model so that the adsorption of Cu^{2+} by Fe^0@DMSN is more suitable for the pseudo-first-order kinetic equation.

To investigate the adsorption capacity of the materials, adsorption isotherms (Fig. 6, *b*) were used to explore the interactions between the toxic heavy metals Cu^{2+} with DMSN and Fe^0@DMSN. The experimental data were tested using Langmuir and Freundlich models, respectively, and the equations for the two isotherm models are expressed as follows:

– Langmuir:

$$\frac{C_e}{q_e}=\frac{1}{q_m K_L}+\frac{C_e}{q_m}; \quad (5)$$

– Freundlich:

$$\ln q_e=\frac{1}{n}\ln C_e+\ln K_F, \quad (6)$$

where C_e (mg·l^{-1}) is the equilibrium concentration of the heavy metal ions; q_e (mg·g^{-1}) is the equilibrium adsorption capacity of the heavy metal ions adsorbed on the adsorbent; q_m (mg·g^{-1}) is the maximum adsorption capacity of the adsorbents; K_L (l·mg^{-1}) and K_F (mg·g^{-1}) are the Langmuir and Freundlich constants, respectively; n is the constant related to the heterogeneity of the adsorbent sites [23].

The correlation parameters of the fitting results are shown in Table 3.

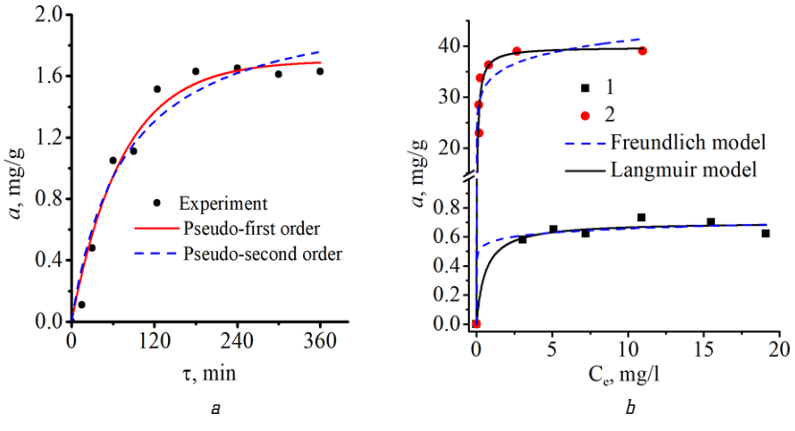

a *b*

Fig. 6. Results of adsorption of Cu^{2+} by of the investigated samples: *a* – adsorption kinetics of Cu^{2+} by of Fe^0@DMSN; *b* – adsorption isotherms of Cu^{2+} by of the investigated samples (T=298 K, pH=5.7±0.1): 1 – DMSN, 2 – Fe^0@DMSN

Table 2

Kinetic parameters of Cu(II) adsorption on Fe^0@DMSN

Sample	Pseudo-first-order			Pseudo-second-order		
	q_e (mg·g^{-1})	K_1 (min^{-1})	R^2	q_e (mg·g^{-1})	K_2 (g·mg^{-1}·min^{-1})	R^2
Fe^0@DMSN	1.700	0.0136	0.972	2.129	0.0062	0.951

Table 3

Fitting parameters for Cu^{2+} adsorption removal isotherms for DMSN and Fe^0@DMSN

Sample	Langmuir			Freundlich		
	q_m (mg·g^{-1})	K_L (l·mg^{-1})	R^2	K_F (mg·g^{-1})	n	R^2
DMSN	0.702	1.754	0.969	0.567	15.73	0.963
Fe^0@DMSN	39.804	12.720	0.955	33.76	11.71	0.922

The Langmuir model for the correlation coefficients of the two adsorbents (R^2 respectively DMSN > 0.97 and Fe^0@DMSN > 0.96) fitted better with the experimental data as compared to the Freundlich model. This indicates that the adsorption process of heavy metal ions on both adsorbents is the same for homogeneous adsorption. The results of calculating the maximum adsorption (q_m) of Cu^{2+} on both adsorbent materials based on the Langmuir model showed that the adsorption capacity of DMSN for Cu ions was insignificant at around 0.7 mg·g^{-1}. However, after Fe^0 modification on its surface, the maximum adsorption of Cu^{2+} by the composite material Fe^0@DMSN increased significantly to 39.8 mg·g^{-1}, which is nearly 57 times higher than that of the adsorption of the initial DMSN material. This confirms our view that Fe^0, as a newly introduced adsorption active site, significantly enhances the adsorption properties of the DMSN substrate for Cu^{2+}.

Limitation of the study: in order to implement the research results in practice, it is necessary to develop a technology for obtaining granular materials using the obtained powder-like adsorbents, which will significantly increase their manufacturability. But, at the same time, on the one hand, the separation of the spent adsorbent from the solution is significantly simplified, and on the other hand, the adsorption capacity of the granules decreases due to the reduction of the specific surface area.

Prospects for further research: in further research, it is necessary to focus attention on improving the structural and sorption characteristics of granular materials and the selectivity of the obtained adsorbents. In addition, it is important to investigate the features of removing heavy metal ions from real industrial wastewater, which contains a complex mixture of pollutants, and to study the possibility of regenerating the spent material for its reuse.

4. Conclusions

In summary, in this study, Fe^0@DMSN composite adsorbent was successfully synthesized by reducing Fe^{3+} ion solution which contained DMSN material with sodium borohydride solution under a nitrogen environment. The material characterization confirmed that the material possessed a solid structure and abundant adsorption functional groups. In addition, its adsorption capacity for the toxic heavy metal Cu^{2+} in simulated wastewater was tested. The adsorption results showed that at pH = 5.7 ± 0.1 and 298 K, the maximum adsorption capacity was 39.8 mg·g^{-1}, which was about 57 times higher than that of the base DMSN material (0.7 mg·g^{-1}), and the kinetic process was described by a pseudo-first-order model. In addition, the adsorbed mixture could utilize an external magnetic field to achieve solid-liquid separation. All the results show that the Fe^0@DMSN composite adsorbent is a promising adsorbent for the treatment of Cu^{2+}-polluted wastewater.

Conflict of interest

The authors declare that they have no conflict of interest in relation to this study, including financial, personal, authorship, or any other, that could affect the study and its results presented in this article.

Financing

The research was performed without financial support.

Data availability

The manuscript has no associated data.

Use of artificial intelligence

The authors confirm that they did not use artificial intelligence technologies when creating this work.

References

1. Zamora-Ledezma, C., Negrete-Bolagay, D., Figueroa, F., Zamora-Ledezma, E., Ni, M., Alexis, F., Guerrero, V. H. (2021). Heavy metal water pollution: A fresh look about hazards, novel and conventional remediation methods. *Environmental Technology & Innovation, 22,* 101504. https://doi.org/10.1016/j.eti.2021.101504
2. Jiang, J., Wang, X., Ren, H., Cao, G., Xie, G., Xing, D., Liu, B. (2020). Investigation and fate of microplastics in wastewater and sludge filter cake from a wastewater treatment plant in China. *Science of The Total Environment, 746,* 141378. https://doi.org/10.1016/j.scitotenv.2020.141378
3. Gao, J., Zhang, L., Liu, S., Liu, X. (2022). Enhanced adsorption of copper ions from aqueous solution by two-step DTPA-modified magnetic cellulose hydrogel beads. *International Journal of Biological Macromolecules, 211,* 689–699. https://doi.org/10.1016/j.ijbiomac.2022.05.073
4. Krstić, V., Urošević, T., Pešovski, B. (2018). A review on adsorbents for treatment of water and wastewaters containing copper ions. *Chemical Engineering Science, 192,* 273–287. https://doi.org/10.1016/j.ces.2018.07.022
5. Ibrahim, Y., Naddeo, V., Banat, F., Hasan, S. W. (2020). Preparation of novel polyvinylidene fluoride (PVDF)-Tin(IV) oxide (SnO_2) ion exchange mixed matrix membranes for the removal of heavy metals from aqueous solutions. *Separation and Purification Technology, 250,* 117250. https://doi.org/10.1016/j.seppur.2020.117250
6. Shi, X., Duan, Z., Jing Wang, Zhou, W., Jiang, M., Li, T., Ma, H., Zhu, X. (2023). Simultaneous removal of multiple heavy metals using single chamber microbial electrolysis cells with biocathode in the micro-aerobic environment. *Chemosphere, 318,* 137982. https://doi.org/10.1016/j.chemosphere.2023.137982
7. Peydayesh, M., Mohammadi, T., Nikouzad, S. K. (2020). A positively charged composite loose nanofiltration membrane for water purification from heavy metals. *Journal of Membrane Science, 611,* 118205. https://doi.org/10.1016/j.memsci.2020.118205
8. Xiao, Y., Tan, S., Wang, D., Wu, J., Jia, T., Liu, Q. et al. (2020). CeO_2/$BiOIO_3$ heterojunction with oxygen vacancies and Ce^{4+}/Ce^{3+} redox centers synergistically enhanced photocatalytic removal heavy metal. *Applied Surface Science, 530,* 147116. https://doi.org/10.1016/j.apsusc.2020.147116

ISSN 2664-9969

9. Feng, X., Long, R., Wang, L., Liu, C., Bai, Z., Liu, X. (2022). A review on heavy metal ions adsorption from water by layered double hydroxide and its composites. *Separation and Purification Technology, 284,* 120099. https://doi.org/10.1016/j.seppur.2021.120099
10. Gupta, M., Gupta, H., Kharat, D. S. (2018). Adsorption of Cu(II) by low cost adsorbents and the cost analysis. *Environmental Technology & Innovation, 10,* 91–101. https://doi.org/10.1016/j.eti.2018.02.003
11. Rubab, R., Ali, S., Rehman, A. U., Khan, S. A., Khan, A. M. (2021). Templated synthesis of NiO/SiO_2 nanocomposite for dye removal applications: Adsorption kinetics and thermodynamic properties. *Colloids and Surfaces A: Physicochemical and Engineering Aspects, 615,* 126253. https://doi.org/10.1016/j.colsurfa.2021.126253
12. Zhang, S., Gao, H., Li, J., Huang, Y., Alsaedi, A., Hayat, T. et al. (2017). Rice husks as a sustainable silica source for hierarchical flower-like metal silicate architectures assembled into ultrathin nanosheets for adsorption and catalysis. *Journal of Hazardous Materials, 321,* 92–102. https://doi.org/10.1016/j.jhazmat.2016.09.004
13. Vojoudi, H., Badiei, A., Bahar, S., Mohammadi Ziarani, G., Faridbod, F., Ganjali, M. R. (2017). A new nano-sorbent for fast and efficient removal of heavy metals from aqueous solutions based on modification of magnetic mesoporous silica nanospheres. *Journal of Magnetism and Magnetic Materials, 441,* 193–203. https://doi.org/10.1016/j.jmmm.2017.05.065
14. Shao, P., Liang, D., Yang, L., Shi, H., Xiong, Z., Ding, L. et al. (2020). Evaluating the adsorptivity of organo-functionalized silica nanoparticles towards heavy metals: Quantitative comparison and mechanistic insight. *Journal of Hazardous Materials, 387,* 121676. https://doi.org/10.1016/j.jhazmat.2019.121676
15. Li, S., Li, S., Wen, N., Wei, D., Zhang, Y. (2021). Highly effective removal of lead and cadmium ions from wastewater by bifunctional magnetic mesoporous silica. *Separation and Purification Technology, 265,* 118341. https://doi.org/10.1016/j.seppur.2021.118341
16. Yang, Y., Bernardi, S., Song, H., Zhang, J., Yu, M., Reid, J. C. et al. (2016). Anion Assisted Synthesis of Large Pore Hollow Dendritic Mesoporous Organosilica Nanoparticles: Understanding the Composition Gradient. *Chemistry of Materials, 28 (3),* 704–707. https://doi.org/10.1021/acs.chemmater.5b03963
17. Zhang, K., Xu, L.-L., Jiang, J.-G., Calin, N., Lam, K.-F., Zhang, S.-J. et al. (2013). Facile Large-Scale Synthesis of Monodisperse Mesoporous Silica Nanospheres with Tunable Pore Structure. *Journal of the American Chemical Society, 135 (7),* 2427–2430. https://doi.org/10.1021/ja3116873
18. Gao, F., Lei, C., Liu, Y., Song, H., Kong, Y., Wan, J., Yu, C. (2021). Rational Design of Dendritic Mesoporous Silica Nanoparticles' Surface Chemistry for Quantum Dot Enrichment and an Ultrasensitive Lateral Flow Immunoassay. *ACS Applied Materials & Interfaces, 13 (18),* 21507–21515. https://doi.org/10.1021/acsami.1c02149
19. Shi, L., Lin, Y.-M., Zhang, X., Chen, Z. (2011). Synthesis, characterization and kinetics of bentonite supported nZVI for the removal of Cr(VI) from aqueous solution. *Chemical Engineering Journal, 171 (2),* 612–617. https://doi.org/10.1016/j.cej.2011.04.038
20. Dong, K., Wu, S., Chang, B., Sun, T. (2023). Zero-valent iron supported by dendritic mesoporous silica nanoparticles to purify dye wastewater. *Journal of Environmental Chemical Engineering, 11 (5),* 110434. https://doi.org/10.1016/j.jece.2023.110434
21. Li, H., Si, R., Wang, W., Huang, Y., Xiang, M., Wang, C. et al. (2021). Sulfidated nanoscale zero-valent iron dispersed in dendritic mesoporous silica nanospheres for degrading tetrabromobisphenol A. *Colloids and Surfaces A: Physicochemical and Engineering Aspects, 621,* 126586. https://doi.org/10.1016/j.colsurfa.2021.126586
22. Yu, J., Bondarieva, A., Tobilko, V., Pavlenko, V. (2023). Adsorption removal of Cu(II) using Ni-modified silica gel. *Water and Water Purification Technologies. Scientific and Technical News, 37 (3),* 3–12.
23. Choi, W. S., Lee, H.-J. (2022). Nanostructured Materials for Water Purification: Adsorption of Heavy Metal Ions and Organic Dyes. *Polymers, 14 (11),* 2183. https://doi.org/10.3390/polym14112183

Junjie Yu, *PhD Student, Department of Chemical Technology of Ceramics and Glass, National Technical University of Ukraine "Igor Sikorsky Kyiv Polytechnic Institute", Kyiv, Ukraine, ORCID: https://orcid.org/0000-0003-1206-8494*

✉ ***Viktoriia Tobilko,*** *PhD, Associate Professor, Department of Chemical Technology of Ceramics and Glass, National Technical University of Ukraine "Igor Sikorsky Kyiv Polytechnic Institute", Kyiv, Ukraine, e-mail: vtobilko@gmail.com, ORCID: https://orcid.org/0000-0002-1800-948X*

✉ *Corresponding author*